Appeared in Sensors and Actuators B: Chemical, vol. 114, no. 1, pp. 254-262, 30 March 2006

Compliant and Low-cost Humidity Sensors using Nano-porous Polymer Membranes

Bozhi Yang, Burak Aksak, Qiao Lin, and Metin Sitti*

Department of Mechanical Engineering, Carnegie Mellon University, Pittsburgh, PA 15213

ABSTRACT

This paper proposes non-fragile compliant humidity sensors that can be fabricated inexpensively on various types of nano-porous polymer membranes such as polycarbonate, cellulose acetate, and nylon membranes. The sensor contains a pair of interdigitated electrodes deposited on the nano-porous polymer membranes. The resistance and/or capacitance between these electrodes vary at different humidity levels with a very high sensitivity due to the water adsorption (capillary condensation) inside the nano-pores. The proposed sensors are low-cost in both material and fabrication. Due to its compliance, the sensors can be suitable for certain applications such as *in-situ* water leakage detection on roofs, where people can walk on top of them. Testing results demonstrated that the sensor changes resistance within large range of humidity values. For most sensors, the resistance changes from 0.1 GΩ to 2000 GΩ when the relative humidity changes from 39% to 100% at room temperature. It takes about 4-8 minutes for the resistance to reach steady state when the sensor was taken from 100% to 39% relative humidity at the room temperature.

Keywords: Humidity sensor; Nanoporous membrane; Polycarbonate; Shadow mask;

1. INTRODUCTION

Humidity sensors are important for a wide range of applications, such as meteorological services, air conditioning, electronics processing, etc [1]. Generally there are two types of humidity

sensors: resistive and capacitive humidity sensors. Resistive humidity sensors usually consist of a moisture-sensitive, conductive material on an interdigitated gold electrode ceramic substrate. The devices' resistance varies exponentially with variations in relative humidity. Capacitive humidity sensors are based on non-conducting materials, which make up the dielectric of a capacitor. The dielectric constant of the film changes as it absorbs water vapor, varying the sensors capacitance in proportion to the changes in relative humidity.

Nano-pore based humidity sensors can detect the resistance and/or capacitance change with a very high sensitivity due to the water adsorption (capillary condensation) inside the nano-pores [1]. In literature, there are many works related to using alumina and other ceramic nano-pore materials for humidity sensing [1,2]. However, ceramic humidity sensors suffer from insufficient sensitivity, low reversibility, and drift in base resistance with time [4]. In addition, the brittleness makes ceramics not suitable for certain applications such as *in-situ* water leakage detection on roofs where people can walk on top of them. Another common sensor material, polyimide film with roughened surface, has been widely used [3], but they swell with water absorption and have a relatively lower sensitivity. Therefore, in this work, novel compliant and nano-porous polymer materials are proposed as sensing materials for non-fragile and high sensitivity detection.

2. SENSING MATERIALS AND MECHANISM

Polycarbonate (PC), cellulose acetate (CA) and polyester (Nylon) membranes with nano-pores were utilized as the sensing materials and their performances are compared. Figure 1 shows the PC and Nylon membranes that we used. Table 1 shows the properties of these membranes.

All of the three materials are commercially available as inexpensive thin 25-mm-diameter circular membranes. The PC, CA, Nylon membrane has a pore size of 200 nm, 200 nm, 100 nm, respectively. The pore density is 3×10^{8} pores/cm^{2} for PC membrane, and the porosity is 66% and 50% for CA and Nylon membrane, respectively. Interdigitated gold electrodes were fabricated on top of these membranes, and resistance and/or capacitance change of the nanosensor was measured

between the electrodes under different humidity conditions. All the membranes are commercially available from Advantec MFS, Inc., Dublin, CA.

The ability of a porous membrane to sense humidity is based upon ionic conduction [4]. The presence of an adsorbed layer of water at the surface reduces the total sensor impedance due to the increase in the ionic conductivity, as well as the capacitance due to the high dielectric constant of water. An additional advantage of porosity is that at a particular temperature and relative humidity (RH), water condensation occurs in pores up to r in radius given by Kelvin's relation [4]:

$$r = \frac{2\gamma_L V}{RT \log(P/P_s)} \approx \frac{1.08}{\log(P/P_s)} nm$$

where P/P_s is the relative humidity, γ_L is the water surface tension, R is the universal gas constant, T is the temperature in Kelvin, and V is the volume of water. Since capillary condensation enhances the sensing capabilities of a material, pore size distribution has been widely considered to be an important parameter in determining the sensitivity in a particular humidity range. Ideally, the membrane pore size should be comparable to r for enhanced sensing, e.g. r =10nm and 1.6 nm for 90% and 50% relative humidity levels, respectively.

The mechanism for nano-porous membrane humidity sensor is to sense the resistance and/or capacitance change of the nanosensors, which will be measured by interdigitated metal electrodes. The two equivalent circuit models [4] are shown in Figure 2. The circuit in (a) is used when only high frequency semicircle is present and that in (b) is used where the low frequency spur co-exists with the high frequency semicircle. In Figure 2a, only resistance R_1 and capacitance $C_1(\omega)$ change as water is absorbed, while in Figure 2b, the fact that water ions can migrate toward the electrodes is also considered. In this paper, we only measure the DC resistance as a preliminary characterization of the sensors.

3. DESIGN

The sensor is composed of a pair of interdigitated metal electrodes built on top of the porous layer for measuring the resistance or capacitance. The porous layer serves as the moisture-sensitive material. By changing the length of single electrodes, number of electrode pairs, and gap between adjacent electrodes, we can optimize the design of the sensor.

We made five different electrode designs, corresponding to two different fabrication methods. Design A and B have relatively larger dimensions, as shown in Figure 3, and are for first fabrication method. In design A there are 4 pairs of electrodes. The dimensions of electrodes are 10 mm × 0.5 mm and the gap between adjacent electrodes is 2 mm. In design B there are 5 pairs of electrodes. The dimensions of a single electrode are 10 mm × 0.3 mm and the gap between two adjacent electrodes is 1 mm.

Design C, D, and E, as shown in Figure 6 and 7, have relatively smaller dimensions and are for the second fabrication method. In design C, there are 19 pairs of electrodes. The dimensions of electrodes are 13 mm × 0.5 mm with a 0.5 mm gap between electrodes. In design D, there are 9 pairs of electrodes, and the electrode fingers have different lengths. Both the width of a single electrode finger and the gap between adjacent fingers are 0.5 mm. In design E, we put five sensors on a single 25 mm diameter membrane separately to compare their performances and to study the possibility to make a sensor array. All smaller sensors in design E have 9 pairs of electrodes, and have exactly the same shape but their dimensions are scaled.

4. FABRICATION

Since acetone and photoresist developer react with the polymer substrate and make the sensing membrane inactive during photoresist stripping, conventional photolithography is not possible to fabricate the sensor electrodes. Therefore, two other methods were exploited using a shadow mask (or “dry lift-off” technique).

The first method is to use an adhesive paper or sticky gel pack as a dry lift-off mask. To start, we laid out the pattern of the electrodes with a CAD software (CorelDraw10) and the electrode patterns were printed on the adhesive paper or gel pack with an office printer. Then the electrode patterns were cut carefully with knife, and removed. We thus obtain a circular shadow mask with hollow electrode patterns. Then we peeled it off and attached this shadow mask to the sensing membrane. After sputtering the electrodes (50 Å Ti/ 1000 Å Au), the mask was removed with tweezers manually, leaving only the electrode patterns. The whole fabrication process, as shown in figure 4, takes only several hours. This fabrication method works well for large electrode patterns. Figure 5 shows two fabricated sensors.

In the second method, we made deep RIE etched Si structures as the shadow masks, and then performed electrode sputtering with them. To prepare the deep RIE etched Si structures, conventional photolighography was used. Instead of making a chromium mask, a commercial high-resolution printer (3600 dpi) was used to print the electrode patterns on a transparency film. A 13 μm thick AZ4620 photoresist was spin-coated on the Si wafer surface, and standard photolithography was used to pattern the shadow mask. It takes about 6 hour to deep-RIE etch through a 500 um thick Si wafer. The following fabrication process is similar to the process flow in Figure 4.

Si shadow mask is superior to adhesive paper and gel pack masks in the sense that the electrode feature sizes can be made much smaller and it can be reused many times. We have fabricated sensors on different membrane materials using the same Si shadow masks, while the Si structures were still in good condition. It is a better method than using adhesive paper mask if high quantities of sensors are to be fabricated.

Gold electrodes were sputtered on the polymer membranes with the K.J. Lesker Sputtering machine.

Once having the Si shadow masks, one can fabricate tens of sensors within several hours without the need for cleanroom facilities. Therefore the proposed humidity sensors have the potential to compete with other sensors, in terms of low-cost and quick fabrication.

5. TESTING

Estimation and preliminary testing shows the resistances of the sensors are out of the range of conventional digital multimeters (usually 100 MΩ). So we used a simple voltage divider circuit to measure the DC resistance, as shown in Figure 8. During testing interconnect wires were bonded to the sensors' bonding pads through silver paste. The sensor was hung inside a plastic humidity adjustment chamber without touching the wall of the chamber. A commercial humidity sensor (MicroDataLogger MDL03411) with a fast time response was used to monitor/calibrate the chamber humidity. The sensor (R_s) was connected in series to a 100 MΩ resistor R_0. A 10 VDC was applied to both resistors, and V_0 (voltage along the R_0) was measured by a multimeter (Agilent 34401A) with input impedance larger than 10 GΩ. Therefore the resistance of the sensor is:

$$R_s = V_s \cdot \frac{R_0}{V_0} = (10 - V_0) \cdot \frac{R_0}{V_0}$$

Figure 9 shows DC resistance vs. relative humidity for design A and design B device fabricated on polycarbonate membranes at 25 C°. The resistance changes from 150 to 0.3 GΩ, and from 77 to 0.1 GΩ, for design A and B device respectively, when humidity changes from 39% to 100%. Design A device has larger resistance because it has less number of electrode pairs and larger gap between two adjacent electrodes than design B device.

Figure 10 shows DC resistance vs. relative humidity for three design C sensors fabricated on polycarbonate, cellulose acetate, and nylon membranes respectively, at 25 C°. When relative humidity changes from 39% to 100%, the resistance changes from 300 to 2GΩ, 1612 to 26 GΩ, and 1389 to 15 GΩ for polycarbonate, cellulose acetate, and nylon membranes, respectively.

Figure 11 shows the time response of the three design C devices in Figure 10 when they were taken out from a 100% to 39% relative humidity environment at 25 C°. It takes about 4, 5, 8 min to get to steady state for the polycarbonate, cellulose acetate, nylon sensors, respectively.

I-V curve of a design D sensor fabricated on polycarbonate membrane with Si shadow mask has been measured by a HP 4155B Semiconductor Parameter Analyzer at room condition. Voltage applied to the sensor was switched from –1 V to +1 V and current was measured, as shown in Figure 12. The curve shows that the sensor behaves generally ohmic, although there is some evidence for polarization and/or non-ohmic behavior. The resistance of the sensor is about 15 GΩ. The resistance is much smaller than the estimated resistance as certain gold goes underneath the Si shadow mask during sputtering, which consequently increases the conductance.

Experiment results show that the sensors resistance strongly depends on the fabrication and packaging method. During the electrode sputtering, gold may go underneath the Si shadow mask, which can significantly change the total sensor resistance. Therefore even for the same sensor design with same type of membrane, the DC resistance may change a significant amount.

In addition, for design A and B sensors made with adhesive paper shadow mask on thin polycarbonate membranes, we bonded the thin membranes to a glass substrate with double-sided adhesive tapes in order to facilitate peeling off the shadow mask from the membrane after sputtering. The tape may decrease the total resistance and lower the sensitivity. This probably explains why the measured resistance of design A and B sensor are smaller than that of design C device, although design A and B sensors should have larger design resistance by their dimensions. Ideally, the sensor should be free from any substrate for best performance.

Testing of design D and E sensors also shows good sensitivity of resistance change as humidity varies. For improved sensor characterization, better testing equipments and/or better testing methods will be use in the future.

6. MODELING

We made 2D steady state modeling of the different sensor designs with Ansys 7.0. In the simulation, 1V and 0 V voltages were applied to the two electrode pads respectively. The volume resistivities of gold and polycarbonate used in the simulation were $2.21\times10^{-8}\Omega\cdot m$ and $5\times10^{10}\Omega\cdot m$, respectively. The voltage potential field, and the electric current vector filed were obtained. Figure 13 shows the electric potential field and current density vector field of a design A sensor. In addition, we calculated the DC resistance between the two electrodes.

The electric potential field and current density vector field shown in Figure 13 are highly ordered between the adjacent electrode combs. The electric potential on each single electrode is almost the same, because the electric resistivity of gold is about 20 orders of magnitude smaller than that of polycarbonate membrane. Since the length of the electrodes is much larger than the gap between electrodes, the electric conduction between the two electrodes can be roughly taken as one-dimensional, which was confirmed by the Ansys simulation result. We thus can use a one-dimensional model to estimate the resistance between the two electrodes.

With the electric resistivity listed above, we obtained the total resistance between the two electrodes by Ansys, which are about $1.38\times10^{14}\Omega$ for design A and $1.52\times10^{13}\Omega$ for design B, respectively. These resistances by modeling are very close to the theoretic result when taking the electric conduction as one-dimensional, which are $1.43\times10^{14}\Omega$ for design A and $1.75\times10^{13}\Omega$ for design B, respectively.

The modeling resistance using nominal polymer resistivity differs from the measured resistance significantly. One possible explanation is that the actual resistivity of the porous membrane is much smaller than the resistivity used in the modeling. In real case, the membrane material is porous instead of bulk phase. There may already be a considerable amount of water vapor condensed inside the nano-pores at the room condition, thus decreasing the nominal resistivity drastically. In addition, in design A and B sensors fabricated on thin polycarbonate membranes with adhesive

paper shadow mask; we use a double-sided tape to bond the membrane to a glass wafer. This tape could increase the conductance of the sensors significantly.

7. CONCLUSIONS

We generated different designs of the nano-pore based polymer humidity sensors, and successfully fabricated the prototype sensors with two different methods: using adhesive paper and deep-RIE etched Si structure as shadow masks respectively. A simple circuit was designed to measure the DC resistance of the sensors. Testing results show that the DC resistance between electrodes changes with high sensitivity as the relatively humidity changes from 39% to 100%. Simple simulations were made to estimate the electric resistance between the electrodes. The electric potential field and electric current density vector field are obtained and analyzed. In the future, we can improve the characterization of the sensors by measuring both the resistance and the capacitance of the sensors with Wheatstone, series and parallel RC bridges to get the impendence data.

ACKNOWLEDGEMENTS

The author would like to thank Prof. David W. Greve for helping on the sensor characterization. This work was funded by The Pennsylvania Infrastructure Technology Alliance (PITA) Program, Institute of Complex Engineering Systems at the Carnegie Mellon University.

REFERENCES

[1] D.K. An, L.H. Mai, “Surface Effect Humidity Sensor Based on Alumina and Porous Silicon Materials: Some Electrical Parameters, Sensitivity and Internal Noises in Comparison”, Sensors, 2002, Proceedings of IEEE, Vol.1, pp. 633 -640, 2002.

[2] A. Wu, M.J. Brett, "Sensing Humidity using nano-structured SiO Posts: Mechanism and Optimization", Sensors and Materials, Vol. 13, No. 7, pp. 399-431, 2001.

[3] Y.L. Yang, L.H. Lo, et al., "Improvement of Polyimide Capacitive Humidity Sensor by Reactive Ion Etching and Novel Electrode Design", Sensors, 2002, Proceedings of IEEE, Vol. 1, pp.511-514, 2002.

[4] E.C. Dickey, O.K. Varghese, K.G. Ong, et al., "Room Temperature Ammonia and Humidity Sensing Using Highly Ordered Nanoporous Alumina Films", Sensors, Vol. 2, pp. 91-110, 2002.

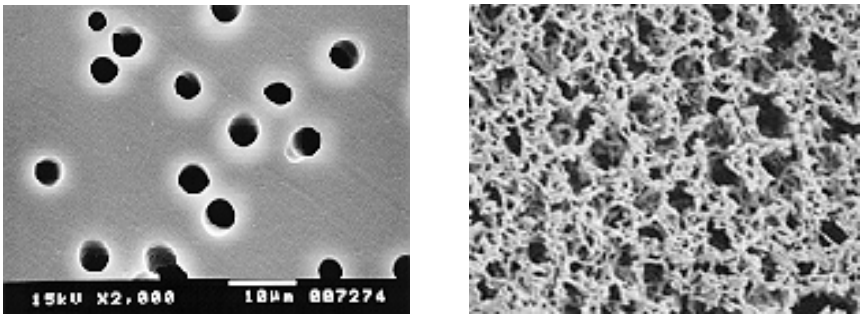

(a) (b)

Figure 1. Micrographs of the two nano-porous sensing materials: (a) polycarbonate and (b) polyester membranes.

Table 1. Properties of three nano-porous polymer membranes.

Membrane material	Resistivity (Ω·cm)	Dielectric Constant at 1MHz	Pore diameter (nm)	Pore density (pores/cm^8) or porosity	Thickness (μm)
Poly-carbonate	5×10^{12}	5	200	3×10^8	10
Cellulose Acetate	10^{14}-10^{16}	2.9	200	66%	125
Nylon	10^{13}	3.4	100	55%	110

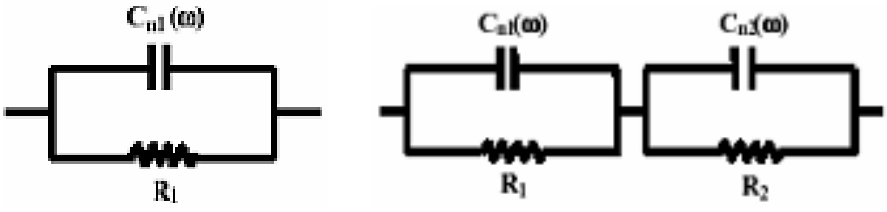

(a) (b)

Figure 2. Equivalent circuits used for fitting experimental data.

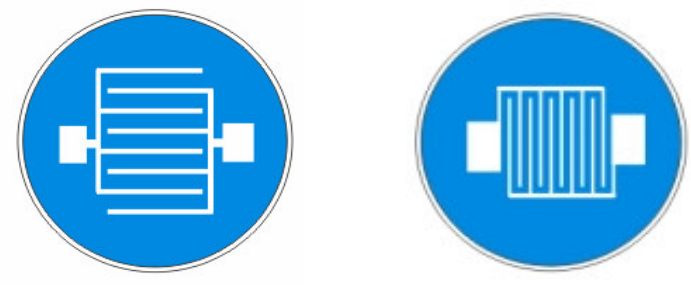

Design A Design B

Figure 3. Design A and design B of humidity sensors. (Diameters are 25 mm for both designs.)

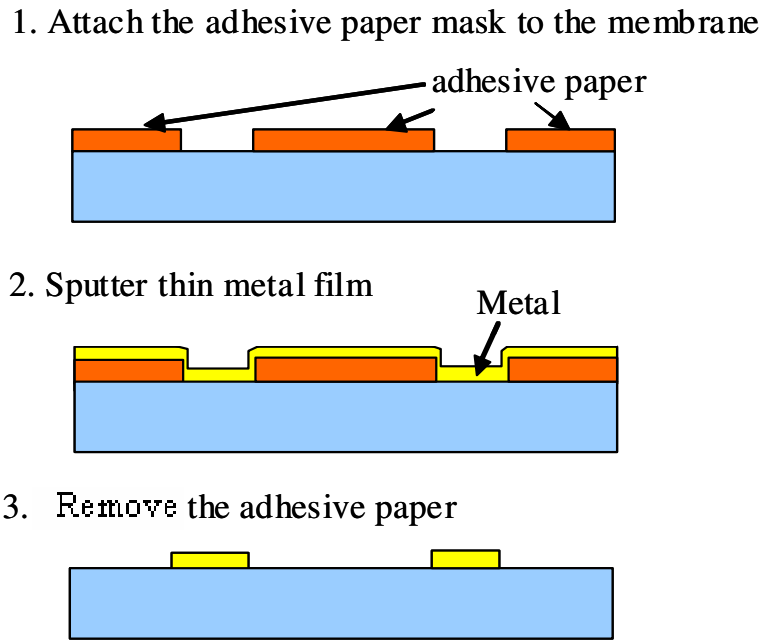

Figure 4. Fabrication process of the humidity sensors using adhesive paper or gel pack as shadow mask.

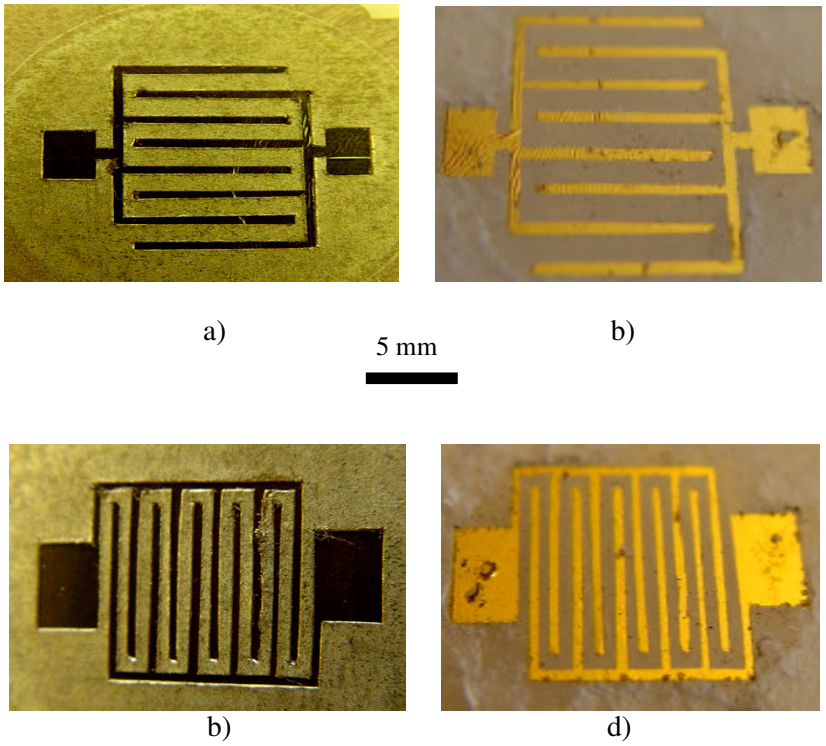

Figure 5. Images of the two humidity sensors fabricated on polycarbonate membranes with adhesive paper shadow masks. a). Design A sensor after sputtering before removing the paper mask. b). Design A device after removing the paper mask. c) and d). Same as a) and b) but for a design B sensor.

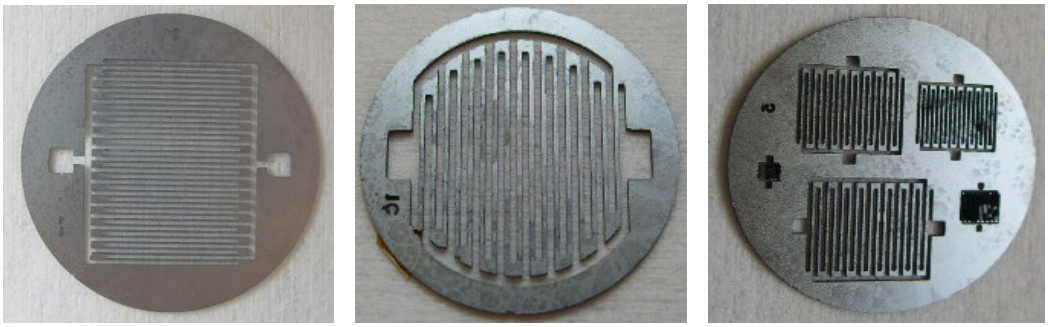

Design C Design D Design E

Figure 6. Si shadow masks fabricated by deep RIE etching of Si with electrode patterns corresponding to design C, D, E. (All Si shadow masks are 26 mm in diameter.)

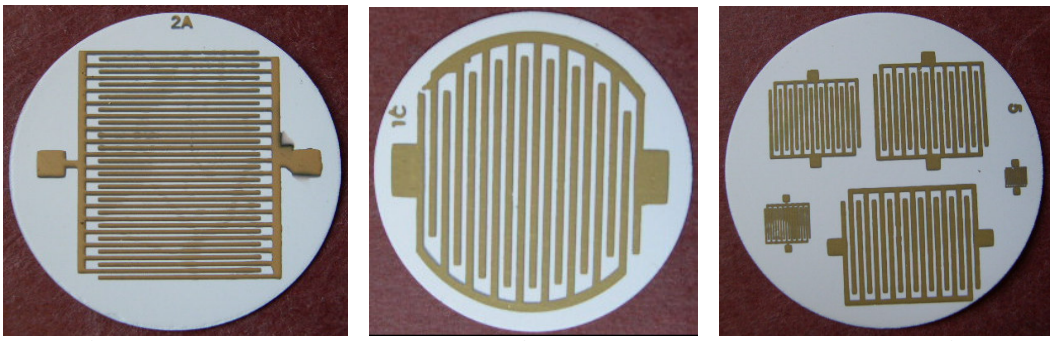

Design C Design D Design E

Figure 7. Images of three sensors fabricated on nano-porous nylon membrane with Si shadow masks, corresponding to design C, D, E. (All membranes are 25 mm in diameter.)

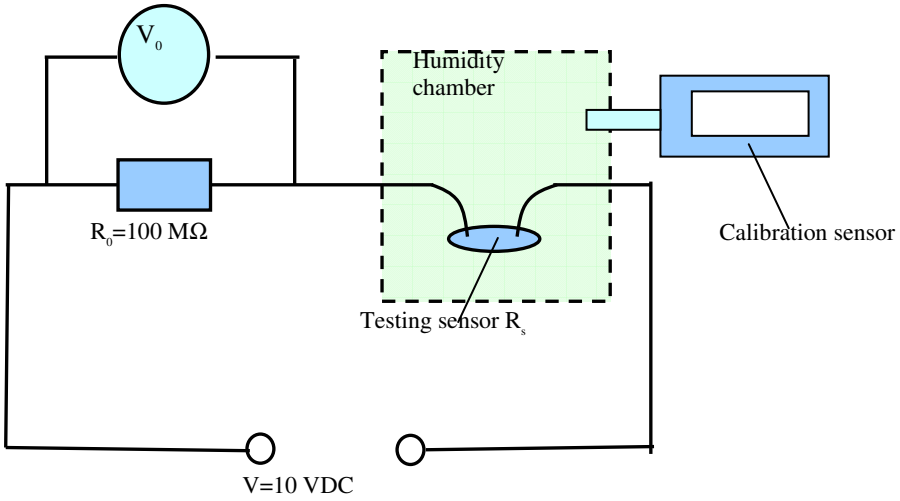

Figure 8. Test setup for the humidity sensors.

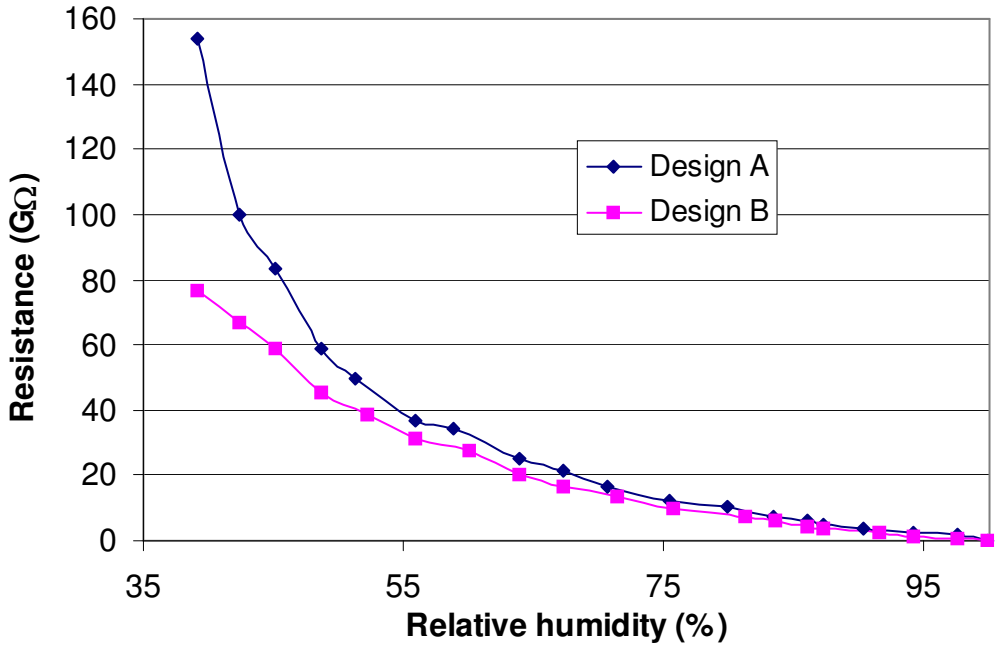

Figure 9. DC resistance vs. relative humidity for design A and B devices fabricated on polycarbonate membranes at 25 C°.

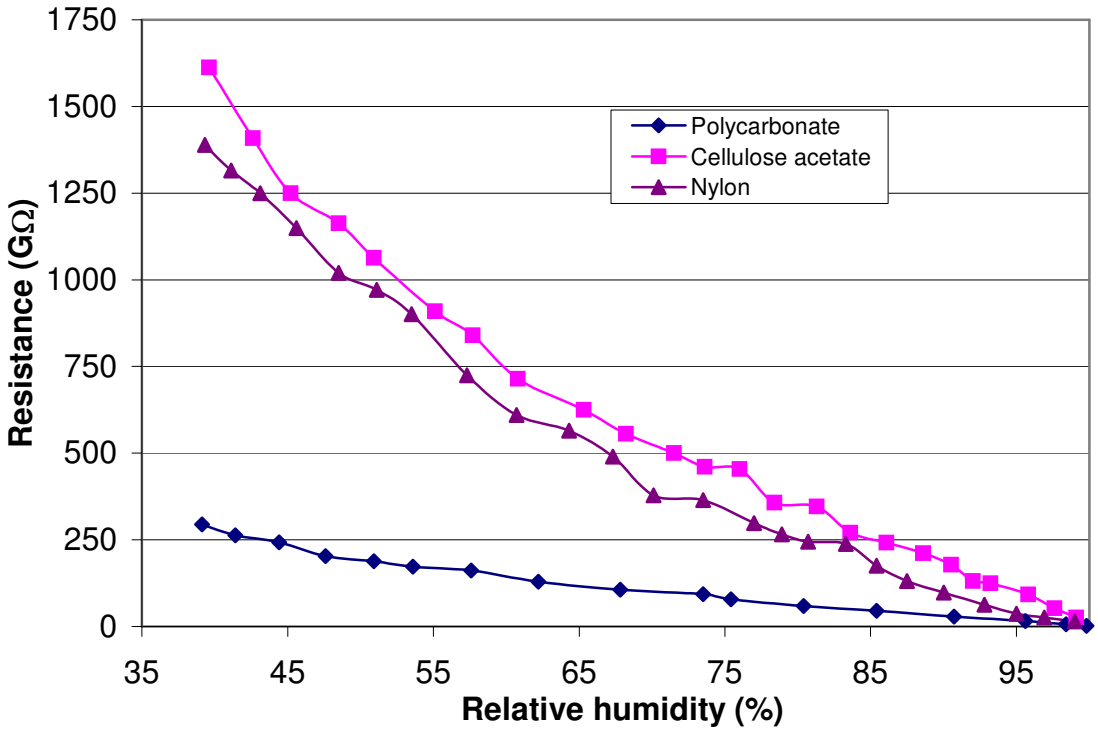

Figure 10. DC resistance vs. relative humidity for three design C devices fabricated on polycarbonate, cellulose acetate, and nylon membranes, respectively, at 25 C°.

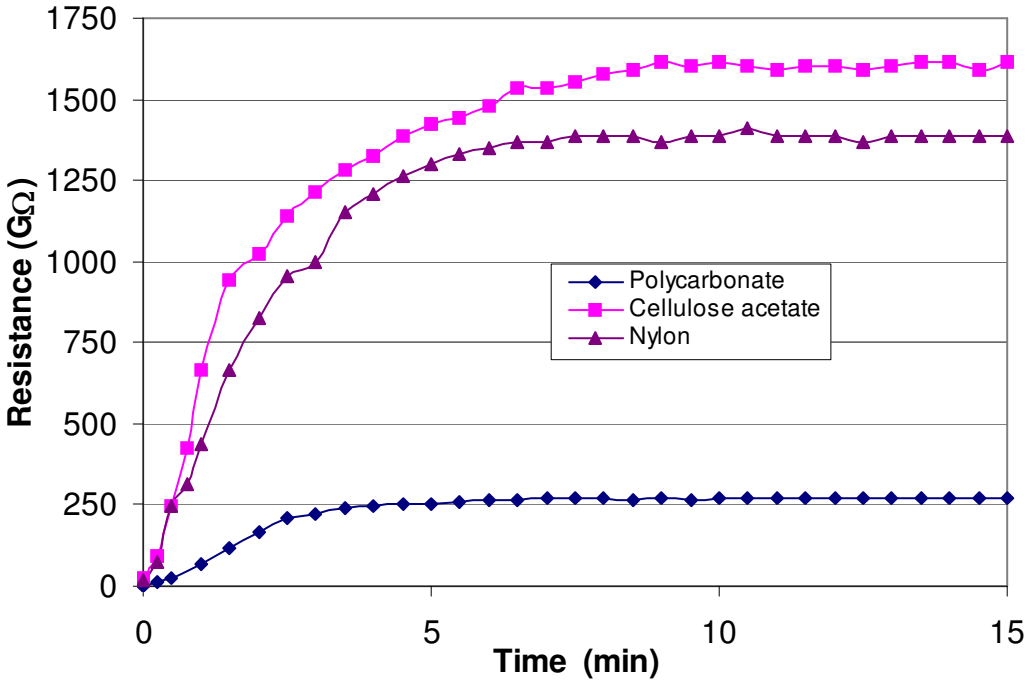

Figure 11. Time response of the three design C devices (in figure 10) when they were taken out from a 100% to 39% relative humidity environment at 25 C°.

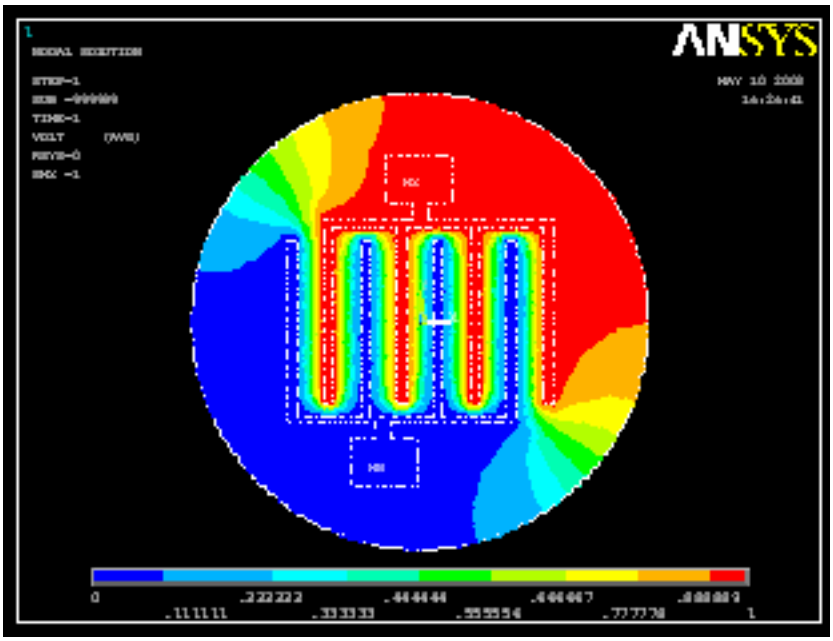

a) Electric potential field

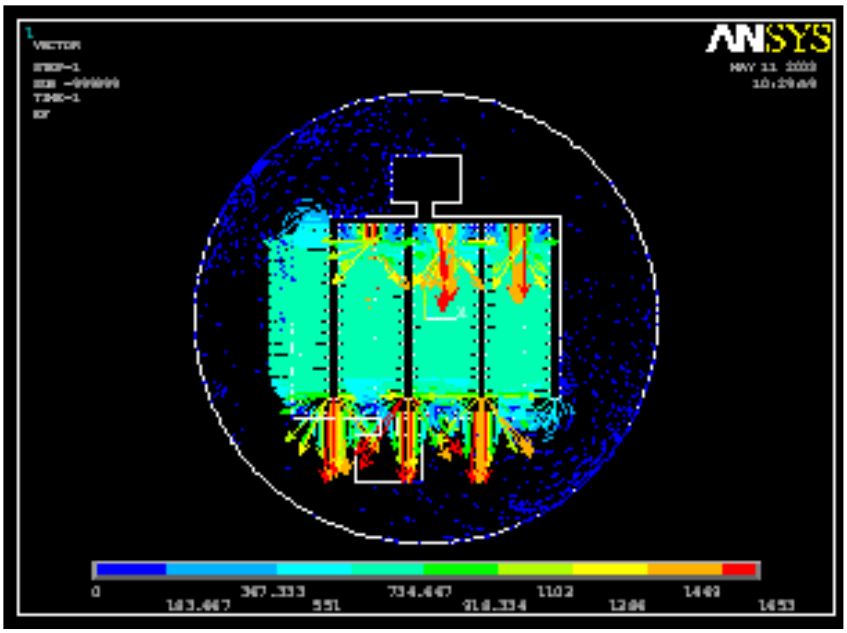

b) Electric current density vector field

Figure 13. Simulated electric potential field and current density vector filed of design B sensor fabricated on a polycarbonate membrane.

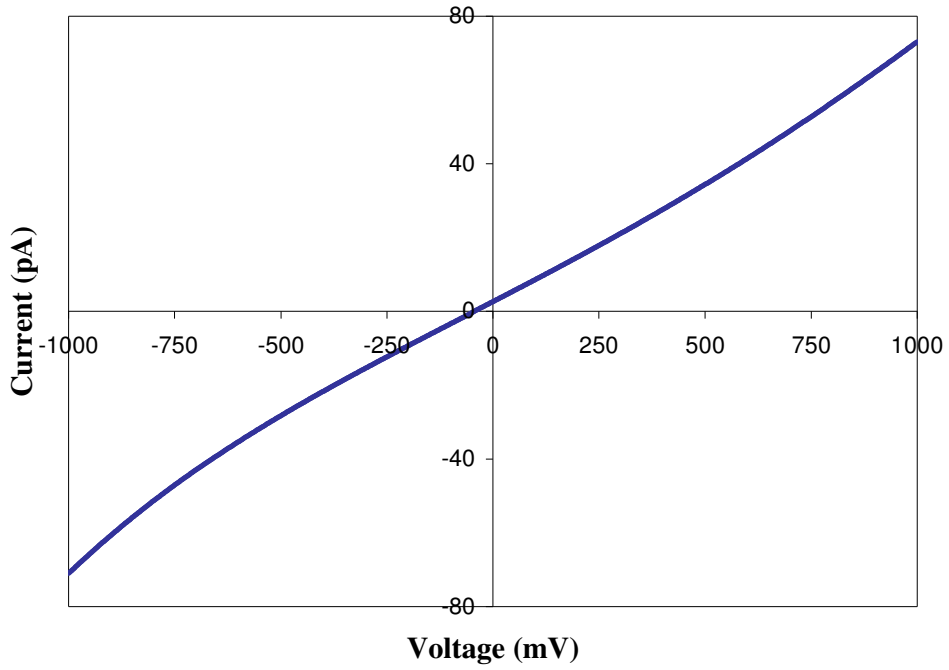

Figure 12. I-V curve of a design D sensor fabricated on polycarbonate membrane.